

1 **The neuroplasticity of division of labor: worker polymorphism, compound eye structure**
2 **and brain organization in the leafcutter ant *Atta cephalotes***

3 Sara Arganda^{1, 2, 3*}

4 Andrew P. Hoadley^{1*}

5 Evan S. Razdan¹

6 Isabella B. Muratore¹

7 James F. A. Traniello^{1,4}

8

9 ¹Department of Biology, Boston University, Boston, USA

10 ²Research Centre on Animal Cognition (CRCA), Centre for Integrative Biology (CBI), Toulouse
11 University, CNRS, UPS, Toulouse 31062, France

12 ³Departamento de Biología y Geología, Física y Química Inorgánica, Área de Biodiversidad y
13 Conservación, Universidad Rey Juan Carlos, Madrid, Spain

14 ⁴Graduate Program for Neuroscience, Boston University, Boston, MA 02215

15

16 * These authors contributed equally to the study

17

18 Dedicated to the memory of Eldridge Adams, brilliant behavioral ecologist, colleague, and
19 friend.

20

21 *Corresponding Author:*

22 S. Arganda

23 ORCID: 0000-0002-9875-2379

24 email: sara.arganda@urjc.es

25 phone: +34 91 488 85 19

26

27

28

29

30

31

32 **Abstract**

33 Our understanding of how the design of peripheral sensory structures is coupled with neural
34 processing capacity to adaptively support division of labor is limited. Workers of the remarkably
35 polymorphic fungus-growing ant *Atta cephalotes* are behaviorally specialized by size: the
36 smallest workers (minims) tend fungi in dark subterranean chambers while larger workers
37 perform tasks mainly outside the nest. These strong differences in worksite light conditions are
38 predicted to influence sensory and processing requirements for vision. We found that eye
39 structure and visual neuropils have been selected to maximize task performance according to
40 light availability. Minim eyes had few ommatidia, large interommatidial angles and eye
41 parameter values, suggesting selection for visual sensitivity over acuity. Large workers had
42 larger eyes with disproportionately more and larger ommatidia, and smaller interommatidial
43 angles and eye parameter values, reflecting peripheral sensory adaptation to ambient rainforest
44 light. Additionally, optic lobe and mushroom body collar volumes were disproportionately small
45 in minims, and within the optic lobe, lamina and lobula relative volumes increased with worker
46 size whereas the medulla decreased. Visual system phenotypes thus correspond to task
47 specializations in dark or light environments and reflect a functional neuroplasticity
48 underpinning division of labor in this socially complex agricultural ant.

49

50 **Keywords (5):** task performance, optic lobe, compound eye, ommatidia, social brain

51

52 **Introduction**

53 Morphology, behavior, and nervous system structure appear to be integrated (Corral-
54 López et al. 2017; Gordon et al. 2017; Iglesias et al. 2018). For example, body size correlates
55 with optical sensitivity and resolution in insect vision (Spaethe and Chittka 2003; Rutowski et al.
56 2009; Palavalli-Nettimi and Narendra 2018; Taylor et al. 2019). Ants are an ideal model system
57 to examine relationships among behavior, body size, and neuroanatomy because workers have
58 evolved as task specialists in several clades (Hölldobler and Wilson 1990). Scaling patterns of
59 brain size and brain compartment substructure among polymorphic workers, moreover, appear to
60 correspond to foraging ecology and the sensory and cognitive demands of task performance
61 (Gronenberg 2008; Muscedere and Traniello 2012; Gordon et al. 2017). Although olfactory
62 inputs are principal information sources in ants (Hölldobler and Wilson 1990; Czaczkes et al.

63 2015), vision can be significant in foraging ecology and navigation (Knaden and Graham 2016;
64 Narendra et al. 2017). To home, foragers may use a celestial compass (Wehner 2003; Muller and
65 Wehner 2006), optic flow (Ronacher and Wehner 1995), visual cues and landmark panoramas
66 (Graham and Cheng 2009; Müller and Wehner 2010; Schwarz et al. 2011; Huber and Knaden
67 2015; Freas et al. 2018), polarized light (Zeil et al. 2014), and canopy patterns (Hölldobler 1980;
68 Beugnon et al. 2005; Rodrigues and Oliveira 2014). Additionally, visual navigation has been
69 associated with peripheral receptor structure, and primary and higher-order processing brain
70 centers (Gronenberg and Hölldobler 1999; Wehner 2003; Ehmer and Gronenberg 2004; Muller
71 and Wehner 2006; Knaden and Graham 2016), and worker behavioral development may be
72 associated with light-exposure and cued neuroanatomical reorganization in the visual system
73 (Stieb et al. 2010, 2012; Yilmaz et al. 2016).

74 Ant ommatidia are photoreceptive units that may change in number and structure
75 according to visual needs (Moser et al. 2004; Narendra et al. 2016a). Ommatidia structure affects
76 visual capacity: larger ommatidia enhance light sensitivity, ommatidia number determine image
77 resolution, and lower interommatidial angle improves acuity (Land 1997). Reproductive and
78 worker division of labor in social insects may have selected for differences in compound eye
79 structure (Schwarz et al. 2011; Streinzer et al. 2013). In some ant species, ommatidia number and
80 size scale with worker body size (Menzel and Wehner 1970; Bernstein and Finn 1971; Klotz et
81 al. 1992; Baker and Ma 2006; Schwarz et al. 2011), vary in males and females (Narendra et al.
82 2016b), and scale differently among polymorphic workers within individual compound eyes and
83 between colonies (Perl and Niven 2016a, b). In bull ants (Greiner et al. 2007; Narendra et al.
84 2011) and bees (Jander and Jander 2002; Greiner et al. 2004) photoreceptor diameter and eye
85 area increase in nocturnal species in comparison to diurnal species, increasing visual sensitivity.
86 Ommatidia facet diameter is generally smaller in diurnal than nocturnal ants (Narendra et al.
87 2017), but eye size patterns vary (e.g. (Menzi 1987)).

88 Visual input from the compound eyes travels to the optic lobes (OL) for primary
89 processing (Gronenberg and Hölldobler 1999). OL investment reflects visual ecology in social
90 insects: in subterranean species, workers are eyeless and OLs are absent whereas diurnal solitary
91 foragers have enormous eyes and their OLs occupy 33% of their brains (Gronenberg and
92 Hölldobler 1999). In paper wasps, queens remain inside the nest and have smaller OLs than
93 foraging workers (O'Donnell et al. 2014), and in the weaver ant *Oecophylla smaragdina*, minor

94 workers nurse brood, rarely leave the nest, and have disproportionately smaller OLs than majors,
95 which forage and defend territory (Kamhi et al. 2017).

96 The OL is comprised of three regions: lamina (contrast detection), medulla (color vision
97 processing and small field motion), and lobula (color vision processing, wide field motion
98 detection, and shape and panorama construction) (Strausfeld 1989; Gronenberg 2008; Dyer et al.
99 2011). OL interneurons project to the collar of the mushroom body (MB) calyx for higher-order
100 processing (Gronenberg 2001; Farris 2016). In ants, males, queens and worker brains show
101 differential investment in the medulla, lobula and MB collar (Ehmer and Gronenberg 2004),
102 reflecting different visual ecologies. Peripheral sensory structure should correlate with higher-
103 order processing ability in task-specialized workers, but this linkage is not well understood.

104 To investigate visual phenotypes within the worker caste, we investigated variation in the
105 structure of the compound eyes, OL, and MB collar in morphologically and behaviorally
106 differentiated workers of the fungus-growing ant *Atta cephalotes*. Worker head widths (HW)
107 range from 0.6 to 4.5mm; this striking polymorphism is associated with the frequency (Wilson
108 1980) and efficiency (Wetterer 1991; van Breda and Stradling 1994) of leaf harvesting, fungal
109 comb maintenance, brood care, hygienic behaviors, and colony defense. The smallest workers
110 (minims, HW<1.2mm) primarily tend brood and the fungal comb in dark underground chambers
111 (Wilson 1980) whereas media workers (HW=1.2-3.0mm) harvest plant material, traveling along
112 foraging trails beneath rainforest canopy, and the largest workers (majors, HW>3.0mm), are
113 responsible for defense (Powell and Clark 2004; Hölldobler and Wilson 2010). Medias use
114 vision during orientation along trails (Vilela et al. 1987; Vick 2005). Size-variable workers thus
115 have different social roles and experience environments strongly differing in ambient light
116 intensity and visual complexity. It is unlikely that a single eye structure and sensory processing
117 ability has evolved in all workers. We hypothesized that *A. cephalotes* visual system
118 organization is associated with the visual ecology of size-related division of labor and has
119 resulted from selection for adaptive plasticity in ommatidia structure, OL organization and MB
120 collar investment. Specifically, we predicted that workers engaging in within-nest or outside-nest
121 activities (in darkness or light, respectively) would vary in compound eye structure and relative
122 investment in the OL and its constituent parts, and in the MB collar to support the requirements
123 of vision associated to task performance.

124

125 **Methods**

126 *Laboratory cultures*

127 Queenright *A. cephalotes* colonies were collected in Trinidad (July 2014) and maintained
128 in a Harris environmental chamber (25°C, 50% relative humidity, 12:12h photoperiod). Artificial
129 nests were constructed from multiple plastic boxes (11cm×18cm×13cm each) connected by
130 plastic tubing (ID=2.5cm). Boxes housing fungal combs had dental stone floors with embedded
131 pebbles to provide air circulation for the fungus. Colonies were fed locally collected leaves free
132 of chemicals and organic produce on alternate days, supplemented with rolled oats, apple, and
133 orange mesocarp.

134 *Worker size variation and tissue sampling*

135 We sampled polymorphic workers from three colonies (Ac09, Ac20, and Ac21). *A.*
136 *cephalotes* appears to exhibit triphasic allometry, with three worker size classes (subcastes):
137 minims (HW across the eyes <1.2mm), medias (HW 1.2-3.0mm) and major workers
138 (HW>3.0mm). Each worker was anesthetized on ice and brains were dissected in ice-cold
139 HEPES buffered saline. Compound eyes were removed and stored in 70% ethanol for
140 processing. Because dissection is delicate, we were not always able to preserve the brain and
141 eyes of the same individual.

142 *Compound eye imaging and structural measurements*

143 Ninety-two intact compound eyes were imaged to create 3D stacks (Fig. 1G) to measure
144 ommatidia number (ON), average ommatidial diameter (D), and interommatidial angle ($\Delta\phi$).
145 Eyes were stored in 70% ethanol, washed in 100% ethanol (3×10 min) before mounting. We
146 measured one eye per worker. Extraneous cuticle was removed to allow eyes to lie flat and were
147 then mounted in methyl salicylate between coverslips and imaged using a Fluoview 1 confocal
148 microscope ($\lambda=488\text{nm}$, step size=3.1 μm) with a 20x air objective (NA=0.5, CA=2). Cuticle has
149 natural fluorescence. Eye data were recorded blind to subcaste by randomly assigning
150 identification numbers to eyes. To quantify ommatidia number, image stacks were flattened in
151 ImageJ (Abràmoff et al. 2004) and facets were counted using the Cell Counter plugin. Volume
152 renderings were viewed in Amira 6.0 to verify counts.

153 Mean ommatidial diameter was calculated from the average diameter of 5 or 10 randomly
154 selected ommatidia from each eye. Eye surface area was calculated from the mean ommatidial
155 diameter (surface area=ON $\times\pi\times[0.5\times D]^2$), and ommatidial density (number of ommatidia per

156 surface area unit) was calculated by dividing the number of ommatidia by eye surface area
157 (Yilmaz et al. 2014). To quantify interommatidial angle ($\Delta\phi$), image stacks were re-sectioned in
158 the yz plane to obtain a virtual cross section of the eye. ImageJ was used to estimate local eye
159 radius R (Schwarz et al. 2011), which with the mean ommatidial diameter (D , in μm) for that
160 eye, interommatidial angle (in radians) could be estimated as $\Delta\phi = D/R$ (Schwarz et al. 2011).
161 Eye parameter (P), which indicates the extent of trade-offs between sensitivity and resolution,
162 was calculated as $\Delta\phi \times D$ (Snyder 1977; Rutowski et al. 2009); lower values of P indicate
163 enhanced acuity, while compromising sensitivity.

164 *Immunohistochemistry and confocal microscopy*

165 After dissection, brains were placed in 16% Zn-formaldehyde (Ott 2008), fixed overnight
166 at approximately 18°C on a shaker, washed in HBS (6×10 min) and then fixed in Dent's Fixative
167 (80% methanol, 20% DMSO) for minimally 1h. Brains were next washed in 100% methanol and
168 either stored at -17°C or immediately processed. Brains were washed in 0.1M Tris buffer
169 (pH=7.4) and blocked in PBSTN (5% neutral goat serum, 0.005% sodium azide in 0.2% PBST)
170 at 18°C for 1 hour before incubation for 3 days at room temperature in primary antibody (1:30
171 SYNORF 1 in PBSTN; monoclonal antibody 3C11 obtained from DSHB, University of Iowa, IA,
172 USA). They were washed (6×10 min) in 0.2% PBST and incubated in secondary antibody (1:100
173 AlexaFluor 488 goat anti-mouse in PBSTN) for 4 days at room temperature. Brains were then
174 washed a final time (6×10 min in 0.2% PBST) and dehydrated in an ethanol series (10min/step,
175 30/50/70/95/100/100% ethanol in 1x PBS), cleared with methyl salicylate, and mounted on
176 stainless steel slides for imaging.

177 Sixty-three brains were imaged using an Olympus Fluoview 1 confocal microscope
178 ($\lambda=488\text{nm}$, step size=3.1 μm) with either a 10x air objective (NA=0.3, CA=1), or a 20x air
179 objective (NA=0.5, CA=2). Voxel depth was multiplied by a factor of 1.59 to correct for axial
180 shortening due to mounting in methyl salicylate (Bucher et al. 2000). Brain image stacks were
181 manually segmented using Amira 6.0 and Amira 2019.2 software to quantify neuropil volumes.
182 Given their bilateral symmetry, we segmented one hemisphere per brain, chosen randomly. Our
183 study goal required that only the lamina, medulla and lobula of the OL and MB calyces
184 (separating lip and collar) were segmented separately (Fig. 2A), the rest of the central brain
185 regions and the suboesophageal ganglion were segmented as a whole. Brain data collection was
186 blind to worker HW, although extreme size differences were obvious. Nevertheless, due the

187 randomized coding of brains, subcaste could not be determined with certainty by the annotator.
188 We calculated the volume of the brain hemisphere, the absolute and relative volume of OL
189 (relative to total brain volume), the absolute and relative volume of MB collar (relative to total
190 brain volume), and the relative volumes of OL subregions (relative to total OL volume).

191 *Statistical evaluation*

192 Statistical evaluations were performed in R (version 3.3.0, Team 2016) using the
193 ‘segmented’ package to analyze eye and brain metric scaling (V. R. M. Muggeo 2008). To assess
194 allometries in eye structure and brain volumes in relation to worker size, least-square means
195 regression was used on log10-transformed values to estimate a and b in the scaling equation
196 $y=aM^b$, as $\log_{10}(y)=\log(a)+b\times\log(M)$. To test the null hypothesis (H_0) of isometry, a separate
197 linear model was calculated and tested against different slope values depending on the metric.
198 The slope for H_0 were $b=0.0$ (linear vs. constant values), $b=1.0$ (linear vs. linear), $b=2.0$ (linear
199 vs. surface area) and $b=3.0$ (linear vs. volume) (Kaspari and Weiser 1999).

200 The Davies test was used to determine if there is a statistically significant change in slope
201 or a ‘breakpoint’ in a linear relationship (Davies 2002). We observed that the significance of
202 some changes in slope depended on a single data point; therefore, we accepted the change in
203 slope only if its significance was always below 0.05 when removing any point from the dataset.
204 The ‘segmented’ package was further used to estimate the location of the breakpoint. If the
205 Davies’ test revealed two piecewise linear relationships in a scaling relationship, least-square
206 means regression was calculated and tested against isometry independently.

207 To further explore whether increased investment in primary visual neuropil might have
208 an impact in higher-order visual processing neuropil, we assessed allometry in the ratio of
209 volumes of the optic lobes and MB collar according to HW. We also calculated a least-square
210 means regression on log10-transformed values and tested against isometry ($b=0.0$).

211

212 **Results**

213 *Eye Structure*

214 The eyes of media and major workers had significantly more ommatidia than minims
215 (Fig. 1A) and showed a significant change in the scaling of ommatidia number and worker size
216 (Davies test, $p<0.001$) at a HW of 1.38mm (95% CI: 1.20 to 1.58mm). Piecewise linear models
217 calculated for both slopes were significant ($p<0.001$, Multiple $R^2=0.989$) with a slope shift from

218 2.03 (95% CI: 1.91 to 2.13) to 1.35 (95% CI: 1.25 to 1.45). Piecewise linear models were also
219 significantly different from isometry ($b=0$; $p<0.001$). Media and major workers also had larger
220 ommatidial diameter (Fig. 1B). The relationship between ommatidial diameter and worker size
221 showed no significant breakpoint (Davies test, $p>0.5$), and these variables were significantly
222 correlated ($F_{(1,90)}=1217$, $p<0.001$, $R^2=0.93$). The slope of the regression line was 0.25 (95% CI:
223 0.24 to 0.27), which was significantly different from isometry ($b=1.0$; $F_{(1,90)}= 1217$, $p<0.001$).

224 Compound eye size (total eye surface area) was correlated with HW (Fig. 1C). Davies' test showed a significant change in the scaling of total eye size and worker size ($p<0.001$) at a
225 HW of 1.44mm (95% CI: 1.20 to 1.72mm). Piecewise linear models calculated for both slopes
226 were found to be significant ($p<0.001$, Multiple $R^2=0.988$) with a slope shift from 2.52 (95% CI:
227 2.36 to 2.68) to 1.84 (95% CI: 1.70 to 1.97). Piecewise linear models were significantly different
228 from isometry ($b=2.0$; $p<0.001$), although the effect size was small.

229 The density of ommatidia decreased with HW (Fig. 1D). The relationship between the
230 density of ommatidia and worker size showed no significant breakpoint (Davies test, $p>0.5$ and
231 these variables showed a significant correlation ($F_{(1,90)}=1217$, $p<0.001$, $R^2=0.93$). The slope was
232 -0.50 (95% CI: -0.53 to -0.48), also significantly different from isometry ($b=0.0$; $F_{(1,90)}= 1217$,
233 $p<0.001$).

234 Interommatidial angle decreased as worker size increased (Fig. 1E). Davies' test for a
235 change in slope showed a significant change in the scaling relationship between interommatidial
236 angle and worker size ($p<0.001$) at a HW of 1.25mm (95% CI: 1.03 to 1.51mm). Piecewise
237 linear models were calculated for both slopes and found to be significant ($p<0.001$, Multiple
238 $R^2=0.84$), with a slope shift from -0.98 (95% CI: -1.21 to -0.76) to -0.33 (95% CI: -0.43 to -
239 0.23). Piecewise linear models were also significantly different from isometry ($b=0$; $p<0.001$).

240 Eye parameter decreased with worker size in minims (Fig. 1F). Davies' test showed a
241 significant change in the scaling relationship between eye parameter and worker size ($p<0.001$)
242 at a HW of 1.26 mm (95% CI: 1.01 to 1.57 mm). Piecewise linear models were calculated for
243 both slopes and found to be significant ($p<0.001$, Multiple $R^2=0.588$) with a slope shift from -
244 0.73 (95% CI: -0.95 to -0.51) to -0.07 (95% CI: -0.20 to 0.05). The first segment of the piecewise
245 linear models was found significantly different from isometry ($b=0$; $p<0.001$), but the second
246 segment was not ($b=0$; $p=0.205$).

247 *Brain Structure*

249 Larger workers had significantly larger brains (Fig. 2B). The relationship between brain
250 volume and worker size showed no significant breakpoint (Davies test, $p>0.05$) and these
251 variables showed a significant positive correlation ($F_{(1,61)}=13.91$, $p<0.001$, $R^2=0.18$) with a slope
252 of 0.37 (95% CI: 0.17 to 0.56) significantly different from isometry ($b=3.0$; $F_{(1,61)}=13.91$,
253 $p<0.001$). We found greater OL investment in media and major workers (Fig. 2C). Relative OL
254 volume and worker size showed a significant positive correlation ($F_{(1,61)}=271.2$, $p<0.001$,
255 $R^2=0.81$) with no significant breakpoint (Davies test, $p=1$). The slope of the regression line was
256 0.76 (95% CI: 0.67 to 0.85) and significantly different from isometry ($b=0.0$; $F_{(1,61)}=271.2$,
257 $p<0.001$).

258 Within the OL, relative investment in lamina increased with worker size (Fig. 2C1).
259 Relative lamina volume and HW showed a significant positive correlation ($F_{(1,61)}=37.77$,
260 $p<0.001$, $R^2=0.37$) with no significant breakpoint (Davies test, $p>0.05$). The slope of the
261 regression line was 0.64 (95% CI: 0.43 to 0.85) and significantly different from isometry ($b=0.0$;
262 $F_{(1,61)}=37.77$, $p<0.001$). Relative investment in the medulla, in contrast, decreased with worker
263 size (Fig. 2C2). Relative medulla volume and HW showed a significant negative correlation
264 ($F_{(1,61)}=51.1$, $p<0.001$, R^2 of 0.45) with no significant breakpoint (Davies test, $p>0.05$) and a
265 slope of -0.17 (95% CI: -0.21 to -0.12), significantly different from isometry ($b=0.0$; $F_{(1,61)}=51.1$,
266 $p<0.001$). Finally, as for the lamina, relative investment in the lobula increased with worker size
267 (Fig. 2C3). Relative lobula volume and HW showed a significant positive correlation
268 ($F_{(1,61)}=13.43$, $p<0.001$, $R^2=0.17$) and no significant breakpoint (Davies test, $p=0.362$). The slope
269 of the regression line was 0.21 (95% CI: 0.10 to 0.32) and significantly different from isometry
270 ($b=0.0$; $F_{(1,61)}=13.43$, $p<0.001$).

271 Media and major workers also invested relatively more in the MB collar (Fig. 2D).
272 Relative collar volume and worker size showed a significant positive correlation ($F_{(1,61)}=13.03$,
273 $p<0.001$, $R^2=0.16$) and no significant breakpoint (Davies test, $p=0.42$). The slope of the
274 regression line was 0.19 (95% CI: 0.08 to 0.29), which was also significantly different from
275 isometry ($b=0.0$; $F_{(1,61)}=13.03$, $p<0.001$). Despite investing more in the MB collar, larger workers
276 had a lower collar:OL volume ratio (Fig. 2E). The relationship between this ratio and worker size
277 showed a significant negative correlation ($F_{(1,61)}=67.17$, $p<0.001$, $R^2=0.52$), no significant
278 breakpoint (Davies test, $p=0.69$), and a slope of -0.57 (95% CI: -0.71 to -0.43), significantly
279 different from isometry ($b=0.0$; $F_{(1,61)}=67.17$, $p<0.001$).

280

281 **Discussion**

282 Social insect compound eyes and visual information processing neuropils enable adaptive
283 behavioral performance according to cognitive challenges of navigation and ambient light levels
284 (Jander and Jander 2002; Mares et al. 2005; Kapustjanskij et al. 2007; Warrant 2008; Narendra et
285 al. 2011, 2016a; Streinzer et al. 2013; Yilmaz et al. 2014; Bulova et al. 2016). Eye size and
286 ommatidia number correlate with worker size in ants, including polymorphic species, and may
287 be associated with task performance (Menzel and Wehner 1970; Klotz and Reid 1992; Schwarz
288 et al. 2011). In polymorphic *A. cephalotes* workers, in which task performance is strongly
289 correlated with body size-related division of labor, differences in worksite sensory ecology
290 appear to select for visual system polyphenism.

291 *Division of labor and eye structure in A. cephalotes*

292 *A. cephalotes* workers perform tasks in the complete darkness of fungal comb chambers
293 and in the filtered light epigaeic environment beneath rainforest canopy. Media workers forage
294 day and night (Cherrett 1968), and use trail pheromones as well. Although olfaction appears to
295 be the dominant sensory modality for foraging in many ants, visual information facilitates trail-
296 following in *Atta laevigata* [69], and other ant species (Beugnon and Fourcassié 1988) alter their
297 use of chemicals or vision depending on light conditions. In *A. cephalotes*, improved forager
298 visual ability may enable flexibility in the use of orientation cues and social signals as ambient
299 light levels change.

300 Minims tend fungi deep underground, medias harvest leaves from their habitat and labor
301 inside the nest, and majors appear to exclusively perform defense and trail maintenance outside.
302 We hypothesized that eye structure variation among subcastes would reflect adaptation to
303 worksite light availability and visual demands for task performance. We expected the eyes of
304 minims to structurally enable light sensitivity over resolution, whereas larger worker eyes were
305 predicted to favor spatial resolution over sensitivity. It is unclear how minims make use of visual
306 information and what level of spatial resolution and sensitivity is needed to work effectively on
307 the fungal comb. Minims, however, also perform some tasks outside the nest, “hitchhiking” on
308 transported leaves during day and night to defend against fly parasites (Linksvayer et al. 2016).
309 We found that the number and size of ommatidia and eye surface area were significantly smaller
310 in minims (Fig. 1A-C), suggesting less capacity to capture light and less reliance on vision to

311 perform their tasks. The larger ommatidia of media and major workers (Fig. 1B) indicate greater
312 sensitivity to light. However, ommatidia size increased hypometrically with body size: although
313 the ommatidia of minims were the smallest, relative ommatidia size was greater in minims than
314 in medias and majors. This may enable minim worker eyes to collect more light than expected
315 from their size, suggesting adaptation to darkness and light (Greiner 2006; Yilmaz et al. 2014).
316 Alternatively, the small size of minim worker eyes and ommatidia may be due to a body size
317 constraint: eye size is as large as developmentally possible to ensure at least a marginal ability to
318 capture light, which may be needed for parasitic fly defenses. Minims also showed a higher
319 density of ommatidia than media and majors (Fig. 1D). Interommatidial angle decreased with
320 worker size, indicating higher visual acuity in larger workers (Fig. 1E). Eye parameter values
321 (Fig. 1F) were significantly higher for minims, but for larger workers, values were lower and not
322 correlated with size. This suggests minim worker eyes are adapted to enhance sensitivity rather
323 than acuity, whereas larger worker eyes structure have been selected for sensitivity and acuity.
324 Higher acuity is adaptive outside the nest, as it allows resolving more distal objects. The
325 significant breakpoints (HW 1.0-1.8mm) found in the linear regressions for ommatidia number,
326 eye surface area, interommatidial angle and eye parameter (Fig. 1A,C,E,F) suggest structural
327 changes to accommodate the body size-associated transition between inside and outside nest
328 division of labor in *A. cephalotes*. Comparisons of eye structure between diurnal, cathemeral,
329 and nocturnal ant (Greiner et al. 2007; Narendra et al. 2013; Yilmaz et al. 2014; Ogawa et al.
330 2019) and bee species (Greiner et al. 2004) are generally consistent with our predictions.

331 Although eye structure determines light sensitivity and visual acuity, other anatomical,
332 physiological, and behavioral adaptations modify visual abilities: variations in the size of
333 rhabdomers (Greiner et al. 2004; Gonzalez-Bellido et al. 2011; Narendra et al. 2017),
334 microsaccadic rhabdomere contractions and microvilli refractory time (Juusola et al. 2016), or
335 pupillary systems mediated by pigment ommatidial cells (Narendra et al. 2013, 2016a) Such
336 visual adaptations in *A. cephalotes* polymorphic workers remain to be studied.

337 *Division of labor and visual neuropil size and structure*

338 In ant species characterized by morphological differentiated subcastes, workers are
339 predicted to vary neurobiologically to support the sensory demands of specialized tasks
340 (Muscедере and Тraniello 2012; Kamhi et al. 2015; Gordon et al. 2019). If metabolic costs
341 associated with the production and maintenance of brains is high, then selection should favor the

342 reduction of neuropil size (e.g.(Aiello and Wheeler 1995; Niven and Laughlin 2008)). We found
343 that brain volume increased with worker size, but larger workers had brains smaller than
344 expected from their body size (Fig. 2A). We expected *A. cephalotes* workers would invest
345 differentially in brain compartments due to their body size-related task repertoires, and found
346 that larger workers had larger eyes and an allometric increase in OL volume (Fig. 2B).
347 Conversely, some diurnal moths have smaller eyes but larger optic lobes than nocturnal species
348 (Stöckl et al. 2016), a pattern also found in analogous brain region in teleost fishes (Iglesias et al.
349 2018). *A. cephalotes* OL were disproportionately larger in larger workers, and consistent with our
350 prediction, minims showed disproportionately less OL investment. This suggests a task-related
351 increasing need for primary visual information processing in larger workers.

352 Our analysis revealed that lamina, medulla and lobula increased with worker size (Fig.
353 S1), maybe due to higher exposure to light in larger workers active outside the nest (as in
354 (Yilmaz et al. 2016)). Within the OLs, larger workers possessed disproportionately larger lamina
355 and lobula, but a disproportionately smaller medulla (Fig. 2C1-C3). These OL subregion
356 allometries suggest that minims might be better at detecting small-field motion whereas larger
357 workers might be better at processing contrast, wide-field motion, shape, and panorama
358 information. This neuroplasticity seems to adaptively support *A. cephalotes* task specialization
359 inside and outside the nest. We also found a disproportional investment in the MB collar in
360 larger workers (Fig. 2D). Enlarged MBs in social hymenopterans might be the result of ancestral
361 neuroanatomical adaptations to process novel visual information [60]. This evolutionary scenario
362 across phylogenetically diverse ant species appears to be reflected in *A. cephalotes* subcastes that
363 vary in visual ecologies. Our results suggest that the increased need for visual cognition in larger
364 workers is greater for primary processing than for higher-order processing. In *Myrmecia* species,
365 nocturnal workers invested relatively less in OL but relatively more in the MB, including the
366 collar, than diurnal workers (Sheehan et al. 2019). Our results showed that minims had the
367 highest collar:optic lobe ratio (Fig. 2E), apparently as an adaptation to performing tasks in
368 darkness. Collaterally, studies of gene expression differences in whole brains of *A. cephalotes*
369 subcastes revealed a significant worker size-related increase in the level of a gene associated
370 with rod cell development, mirroring the higher demand for visual acuity and larger eye
371 structures in larger workers (Muratore et al., unpublished data). This trend was also true for a

372 gene associated with growth factor activity, potentially contributing to the allometric OL
373 enlargement and other brain regions.

374

375 **Conclusions**

376 We found optical and neural plasticity are associated with the complex agrarian division
377 of labor of *A. cephalotes* workers. Previous studies describe differences in eye structure (Menzel
378 and Wehner 1970; Bernstein and Finn 1971; Klotz et al. 1992; Baker and Ma 2006; Schwarz et
379 al. 2011) or visual neuropil investment (O'Donnell et al. 2018). Our results advance our
380 understanding of ant visual system functionality by demonstrating caste-related compound eye
381 and brain plasticity that has evolved in response to worksite light levels. Worker polymorphism
382 has been shown to be correlated with patriline in the several leafcutting ant species (Hughes et al.
383 2003; Evison and Hughes 2011), suggesting a potential link between genetic variation and the
384 neuroanatomical patterns described here. Division of labor underpinning the fungicultural habits
385 of *A. cephalotes* appears to have played an important selective role in worker visual system
386 evolution. Worker behavior in this species, however, depends on visual and olfactory
387 information that likely varies with the cognitive requirements of tasks. The influence of these
388 factors on the spatial resolving power and sensitivity of eyes and macroscopic and cellular
389 structure of *A. cephalotes* brains requires further study.

390

391 **Conflicts of interest/Competing interests**

392 The authors declare that they have no conflict of interest

393

394 **Author's contributions**

395 APH and ESR prepared brains for imaging and registered images; APH, ESR and SA analyzed
396 neuropil volumes; ESR initiated and designed the eye metric imaging protocol, registered eye
397 images, and measured eye structure; APH and SA performed statistical analysis; APH collected
398 ant colonies; IBM analyzed confocal images and contributed to manuscript content; ESR and
399 APH prepared the first draft of the manuscript; JFAT, APH, ESR, and SA conceptualized and
400 designed the study. JFAT secured funding for the study; JFAT and SA wrote the manuscript. All
401 authors edited and approved the final content of the manuscript.

402

403 **Acknowledgments**

404 We are very grateful for the assistance of Dr. Darcy Gordon (study design, scaling analysis, and
405 statistics), Dr. Christopher Starr and Ricardo “Monkey” Pillai (colony collection), Dr. Todd
406 Blute (confocal training), Dr. Alfonso Pérez-Escudero (data analysis and interpretation), and Dr.
407 J. Frances Kamhi (insightful comments on the manuscript). This research was supported by
408 National Science Foundation grant IOS 1354291 to JFAT, a Marie Skłodowska-Curie Individual
409 Fellowship BrainiAnts-660976 and Ayudas destinadas a la atracción de talento investigador a la
410 Comunidad de Madrid en centros de I+D to SAC, the Undergraduate Research Opportunities
411 Program at Boston University to ESR, and a National Science Foundation Graduate Research
412 Fellowship (DGE-1247312) to APH.

413

414 **References**

415 Abràmoff MD, Hospitals I, Magalhães PJ, Abràmoff M (2004) Image Processing with ImageJ.
416 Biophotonics Int 11:36–42

417 Aiello L, Wheeler P (1995) The expensive-tissue hypothesis: the brain and the digestive system
418 in human and primate evolution. Curr Anthropol 36:199–221

419 Baker GT, Ma PWK (2006) Morphology and number of Ommatidia in the compound eyes of
420 *Solenopsis invicta*, *Solenopsis richteri*, and their hybrid (Hymenoptera: Formicidae). Zool
421 Anz 245:121–125. <https://doi.org/10.1016/j.jcz.2006.06.001>

422 Bernstein S, Finn C (1971) Ant compound eye: Size-related ommatidium differences within a
423 single wood ant nest. Experientia 27:708–710. <https://doi.org/10.1007/BF02136977>

424 Beugnon G, Fourcassié V (1988) How do red wood ants orient during diurnal and nocturnal
425 foraging in a three dimensional system? II. Field experiments. Insectes Soc 35:106–124

426 Beugnon G, Lachaud JP, Chagné P (2005) Use of long-term stored vector information in the
427 neotropical ant *Gigantiops destructor*. J Insect Behav 18:415–432.
428 <https://doi.org/10.1007/s10905-005-3700-8>

429 Bucher D, Scholz M, Stetter M, et al (2000) Correction methods for three-dimensional
430 reconstructions from confocal images: I. Tissue shrinking and axial scaling. J Neurosci
431 Methods 100:135–143. [https://doi.org/10.1016/S0165-0270\(00\)00245-4](https://doi.org/10.1016/S0165-0270(00)00245-4)

432 Bulova SJ, Purce K, Khodak P, et al (2016) Into the black and back: the ecology of brain
433 investment in Neotropical army ants (Formicidae: Dorylinae). Sci Nat 103:31.
434 <https://doi.org/DOI 10.1007/s00114-016-1353-4>

435 Cherrett JM (1968) The foraging behaviour of *Atta cephalotes* L. (Hymenoptera, Formicidae). J
436 Anim Ecol 37:387. <https://doi.org/10.2307/2955>

437 Corral-López A, Garate-Olaizola M, Buechel SD, et al (2017) On the role of body size, brain
438 size, and eye size in visual acuity. Behav Ecol Sociobiol 71:179.
439 <https://doi.org/10.1007/s00265-017-2408-z>

440 Czaczkes TJ, Grüter C, Ratnieks FLW (2015) Trail Pheromones, An integrative view of their
441 role in social insect colony organization. Annu Rev Entomol 60:581–599.
442 <https://doi.org/10.1146/annurev-ento-010814-020627>

443 Davies R (2002) Hypothesis testing when a nuisance parameter is present only under the
444 alternative: Linear Model Case. *Biometrika* 89:484–489

445 Dyer AG, Paulk AC, Reser DH (2011) Colour processing in complex environments: Insights
446 from the visual system of bees. *Proc R Soc B Biol Sci* 278:952–959.
447 <https://doi.org/10.1098/rspb.2010.2412>

448 Ehmer B, Gronenberg W (2004) Mushroom body volumes and visual interneurons in ants:
449 comparison between sexes and castes. *J Comp Neurol* 469:198–213.
450 <https://doi.org/10.1002/cne.11014>

451 Evison SEF, Hughes WOH (2011) Genetic caste polymorphism and the evolution of polyandry
452 in *Atta* leaf-cutting ants. *Naturwissenschaften* 98:643–649. <https://doi.org/10.1007/s00114-011-0810-3>

454 Farris SM (2016) Insect societies and the social brain. *Curr Opin Insect Sci* 1–8.
455 <https://doi.org/10.1016/j.cois.2016.01.010>

456 Freas CA, Wystrach A, Narendra A, Cheng K (2018) The view from the trees: Nocturnal bull
457 ants, *Myrmecia midas*, use the surrounding panorama while descending from trees. *Front*
458 *Psychol* 9:1–15. <https://doi.org/10.3389/fpsyg.2018.00016>

459 Gonzalez-Bellido PT, Wardill TJ, Juusola M (2011) Compound eyes and retinal information
460 processing in miniature dipteran species match their specific ecological demands. *Proc Natl*
461 *Acad Sci U S A* 108:4224–4229. <https://doi.org/10.1073/pnas.1014438108>

462 Gordon DG, Ilieş I, Traniello JFA (2017) Behavior, brain, and morphology in a complex insect
463 society: trait integration and social evolution in the exceptionally polymorphic ant *Pheidole*
464 *rhea*. *Behav Ecol Sociobiol* 71:166. <https://doi.org/10.1007/s00265-017-2396-z>

466 Gordon DG, Zelaya A, Arganda-Carreras I, et al (2019) Division of labor and brain evolution in
467 insect societies: Neurobiology of extreme specialization in the turtle ant *Cephalotes varians*.
468 *PLoS One* 14:1–16. <https://doi.org/10.1371/journal.pone.0213618>

469 Graham P, Cheng K (2009) Ants use the panoramic skyline as a visual cue during navigation.
470 *Curr Biol* 19:R935–R937. <https://doi.org/10.1016/j.cub.2009.08.015>

471 Greiner B (2006) Adaptations for nocturnal vision in insect apposition eyes. *Int Rev Cytol*
472 250:1–46. [https://doi.org/10.1016/S0074-7696\(06\)50001-4](https://doi.org/10.1016/S0074-7696(06)50001-4)

473 Greiner B, Narendra A, Reid SF, et al (2007) Eye structure correlates with distinct foraging-bout
474 timing in primitive ants. *Curr Biol* 17:879–880. <https://doi.org/10.1016/j.cub.2007.08.015>

475 Greiner B, Ribi WA, Warrant EJ (2004) Retinal and optical adaptations for nocturnal vision in
476 the halictid bee *Megalopta genalis*. *Cell Tissue Res* 316:377–390.
477 <https://doi.org/10.1007/s00441-004-0883-9>

478 Gronenberg W (2008) Structure and function of ant (Hymenoptera: Formicidae) brains: strength
479 in numbers. *Myrmecol News* 11:25–36

480 Gronenberg W (2001) Subdivisions of hymenopteran mushroom body calyces by their afferent
481 supply. *J Comp Neurol* 435:474–489. <https://doi.org/10.1002/cne.1045>

482 Gronenberg W, Hölldobler B (1999) Morphologic representation of visual and antennal
483 information in the ant brain. *J Comp Neurol* 412:229–240.
484 [https://doi.org/10.1002/\(SICI\)1096-9861\(19990920\)412:2<229::AID-CNE4>3.0.CO;2-E](https://doi.org/10.1002/(SICI)1096-9861(19990920)412:2<229::AID-CNE4>3.0.CO;2-E)

485 Hölldobler B (1980) Canopy orientation : a new kind of orientation in ants. *Science* (80-)
486 210:86–88

487 Hölldobler B, Wilson EO (2010) The leafcutter ants: civilization by instinct. WW Norton &
488 Company

489 Hölldobler B, Wilson EO (1990) *The Ants*. Harvard University Press, Cambridge, MA
490 Huber R, Knaden M (2015) Egocentric and geocentric navigation during extremely long
491 foraging paths of desert ants. *J Comp Physiol A Neuroethol Sensory, Neural, Behav Physiol*
492 201:609–616. <https://doi.org/10.1007/s00359-015-0998-3>
493 Hughes WOH, Sumner S, Van Borm S, Boomsma JJ (2003) Worker caste polymorphism has a
494 genetic basis in *Acromyrmex* leaf-cutting ants. *Proc Natl Acad Sci U S A* 100:9394–9397.
495 <https://doi.org/10.1073/pnas.1633701100>
496 Iglesias TL, Dornburg A, Warren DL, et al (2018) Eyes Wide Shut: the impact of dim-light
497 vision on neural investment in marine teleosts. *J Evol Biol* 31:1082–1092.
498 <https://doi.org/10.1111/jeb.13299>
499 Jander U, Jander R (2002) Allometry and resolution of bee eyes (Apoidea). *Arthropod Struct
500 Dev* 30:179–193. [https://doi.org/10.1016/S1467-8039\(01\)00035-4](https://doi.org/10.1016/S1467-8039(01)00035-4)
501 Juusola M, Dau A, Song Z, et al (2016) Microsaccadic information sampling provides
502 *Drosophila* hyperacute vision. *Elife* 6:e26117. <https://doi.org/10.7554/elife.26117>
503 Kamhi JF, Nunn K, Robson SKA, Traniello JFA (2015) Polymorphism and division of labour in
504 a socially complex ant: neuromodulation of aggression in the Australian weaver ant,
505 *Oecophylla smaragdina*. *Proc Biol Sci* 282:20150704-.
506 <https://doi.org/10.1098/rspb.2015.0704>
507 Kamhi JF, Sandridge-Gresko A, Walker C, et al (2017) Worker brain development and colony
508 organization in ants: Does division of labor influence neuroplasticity? *Dev Neurobiol*
509 77:1072–1085. <https://doi.org/10.1002/dneu.22496>
510 Kapustjanskij A, Streinzer M, Paulus HF, Spaethe J (2007) Bigger is better: Implications of body
511 size for flight ability under different light conditions and the evolution of alloethism in
512 bumblebees. *Funct Ecol* 21:1130–1136. <https://doi.org/10.1111/j.1365-2435.2007.01329.x>
513 Kaspari M, Weiser MD (1999) The size–grain hypothesis and interspecific scaling in ants.
514 *Fuctional Ecol* 13:530–538. <https://doi.org/10.1046/j.1365-2435.1999.00343.x>
515 Klotz JH, Reid BL (1992) The use of spatial cues for structural guideline orientation in
516 *Tapinoma sessile* and *Camponotus pennsylvanicus* (Hymenoptera: Formicidae). *J Insect
517 Behav* 5:71–82. <https://doi.org/10.1007/BF01049159>
518 Klotz JH, Reid BL, Gordon WC (1992) Variation of ommatidia number as a function of worker
519 size in *Camponotus pennsylvanicus* (DeGeer) (Hymenoptera: Formicidae). *Insectes Soc*
520 39:233–236. <https://doi.org/10.1007/BF01249297>
521 Knaden M, Graham P (2016) The sensory ecology of ant navigation: from natural environments
522 to neural mechanisms. *Annu Rev Entomol* 61:63–76. <https://doi.org/10.1146/annurev-ento-010715-023703>
524 Land MF (1997) Visual Acuity in Insects. *Annu Rev Entomol* 42:147–177.
525 <https://doi.org/10.1146/annurev.ento.42.1.147>
526 Linksvayer TA, Mccall AC, Jensen RM, et al (2016) The function of hitchhiking behavior in the
527 leaf-cutting ant *Atta cephalotes*. *Biotropica* 34:93–100. <https://doi.org/10.1111/j.1744-7429.2002.tb00245.x>
529 Mares S, Ash L, Gronenberg W (2005) Brain allometry in bumblebee and honey bee workers.
530 *Brain Behav Evol* 66:50–61. <https://doi.org/10.1159/000085047>
531 Menzel R, Wehner R (1970) Augenstrukturen bei verschiedenen großen Arbeiterinnen von
532 *Cataglyphis bicolor* Fabr. (Formicidae, Hymenoptera). *Z Vgl Physiol* 68:446–449.
533 <https://doi.org/10.1007/BF00297741>
534 Menzi U (1987) Visual adaptation in nocturnal and diurnal ants. *J Comp Physiol A* 160:11–21.

535 https://doi.org/10.1007/BF00613437
536 Moser JC, Reeve JD, Bento JMS, et al (2004) Eye size and behaviour of day- and night-flying
537 leafcutting ant alates. *J Zool* 264:69–75. <https://doi.org/10.1017/S0952836904005527>
538 Muller M, Wehner R (2006) The significance of direct sunlight and polarized skylight in the
539 ant's celestial system of navigation. *Proc Natl Acad Sci* 103:12575.
540 <https://doi.org/10.1073/pnas.0604430103>
541 Müller M, Wehner R (2010) Path integration provides a scaffold for landmark learning in desert
542 ants. *Curr Biol* 20:1368–1371. <https://doi.org/10.1016/j.cub.2010.06.035>
543 Muscedere ML, Traniello JFA (2012) Division of labor in the hyperdiverse ant genus *Pheidole* is
544 associated with distinct subcaste-and age-related patterns of worker brain organization.
545 *PLoS One* 7:e31618. <https://doi.org/10.1371/journal.pone.0031618>
546 Narendra A, Alkaladi A, Raderschall CA, et al (2013) Compound eye adaptations for diurnal and
547 nocturnal lifestyle in the intertidal ant, *Polyrhachis sokolova*. *PLoS One* 8:e76015.
548 <https://doi.org/10.1371/journal.pone.0076015>
549 Narendra A, Greiner B, Ribi WA, Zeil J (2016a) Light and dark adaptation mechanisms in the
550 compound eyes of *Myrmecia* ants that occupy discrete temporal niches. *J Exp Biol*
551 219:2435–2442. <https://doi.org/10.1242/jeb.142018>
552 Narendra A, Kamhi JF, Ogawa Y (2017) Moving in dim light: behavioral and visual adaptations
553 in nocturnal ants. *Integr Comp Biol* 57:1104–1116. <https://doi.org/10.1093/icb/icx096>
554 Narendra A, Ramirez-Esquivel F, Ribi WA (2016b) Compound eye and ocellar structure for
555 walking and flying modes of locomotion in the Australian ant, *Camponotus consobrinus*.
556 *Sci Rep* 6:1–10. <https://doi.org/10.1038/srep22331>
557 Narendra A, Reid SF, Greiner B, et al (2011) Caste-specific visual adaptations to distinct daily
558 activity schedules in Australian *Myrmecia* ants. *Proc R Soc B Biol Sci* 278:1141–1149.
559 <https://doi.org/10.1098/rspb.2010.1378>
560 Niven JE, Laughlin SB (2008) Energy limitation as a selective pressure on the evolution of
561 sensory systems. *J Exp Biol* 211:1792–804. <https://doi.org/10.1242/jeb.017574>
562 O'Donnell S, Bulova S, Barrett M, Von Beeren C (2018) Brain investment under colony-level
563 selection: Soldier specialization in *Eciton* army ants (Formicidae: Dorylinae). *BMC Zool*
564 3:1–6. <https://doi.org/10.1186/s40850-018-0028-3>
565 O'Donnell S, Clifford MR, Bulova SJ, et al (2014) A test of neuroecological predictions using
566 paperwasp caste differences in brain structure (Hymenoptera: Vespidae). *Behav Ecol
567 Sociobiol* 68:529–536. <https://doi.org/10.1007/s00265-013-1667-6>
568 Ogawa Y, Ryan LA, Palavalli-Nettimi R, et al (2019) Spatial resolving power and contrast
569 sensitivity are adapted for ambient light conditions in Australian *Myrmecia* ants. *Front Ecol
570 Evol* 7:1–10. <https://doi.org/10.3389/fevo.2019.00018>
571 Ott SR (2008) Confocal microscopy in large insect brains: Zinc-formaldehyde fixation improves
572 synapsin immunostaining and preservation of morphology in whole-mounts. *J Neurosci
573 Methods* 172:220–230. <https://doi.org/10.1016/j.jneumeth.2008.04.031>
574 Palavalli-Nettimi R, Narendra A (2018) Miniaturisation decreases visual navigational
575 competence in ants. *J Exp Biol* 221:jeb177238. <https://doi.org/10.1242/jeb.177238>
576 Perl CD, Niven JE (2016a) Colony-level differences in the scaling rules governing wood ant
577 compound eye structure. *Sci Rep* 6:1–8. <https://doi.org/10.1038/srep24204>
578 Perl CD, Niven JE (2016b) Differential scaling within an insect compound eye. *Biol Lett* 12:0–3.
579 <https://doi.org/10.1098/rsbl.2016.0042>
580 Powell S, Clark E (2004) Combat between large derived societies: A subterranean army ant

581 established as a predator of mature leaf-cutting ant colonies. *Insectes Soc* 51:342–351.
582 <https://doi.org/10.1007/s00040-004-0752-2>

583 Rodrigues PAP, Oliveira PS (2014) Visual navigation in the Neotropical ant *Odontomachus*
584 *hastatus* (Formicidae, Ponerinae), a predominantly nocturnal, canopy-dwelling predator of
585 the Atlantic rainforest. *Behav Processes* 109:48–57.
586 <https://doi.org/10.1016/j.beproc.2014.06.007>

587 Ronacher B, Wehner R (1995) Desert ants *Cataglyphis fortis* use self-induced optic flow to
588 measure distances travelled. *J Comp Physiol A* 177:21–27.
589 <https://doi.org/10.1007/BF00243395>

590 Rutowski RL, Gislén L, Warrant EJ (2009) Visual acuity and sensitivity increase allometrically
591 with body size in butterflies. *Arthropod Struct Dev* 38:91–100.
592 <https://doi.org/10.1016/j.asd.2008.08.003>

593 Schwarz S, Narendra A, Zeil J (2011) The properties of the visual system in the Australian desert
594 ant *Melophorus bagoti*. *Arthropod Struct Dev* 40:128–134.
595 <https://doi.org/10.1016/j.asd.2010.10.003>

596 Sheehan ZBV, Kamhi JF, Seid MA, Narendra A (2019) Differential investment in brain regions
597 for a diurnal and nocturnal lifestyle in Australian *Myrmecia* ants. *J Comp Neurol* 527:1261–
598 1277. <https://doi.org/10.1002/cne.24617>

599 Snyder AW (1977) Acuity of compound eyes: Physical limitations and design. *J Comp Physiol*
600 A 116:161–182. <https://doi.org/10.1007/BF00605401>

601 Spaethe J, Chittka L (2003) Interindividual variation of eye optics and single object resolution in
602 bumblebees. *J Exp Biol* 206:3447–3453. <https://doi.org/10.1242/jeb.00570>

603 Stieb SM, Hellwig A, Wehner R, Rössler W (2012) Visual experience affects both behavioral
604 and neuronal aspects in the individual life history of the desert ant *Cataglyphis fortis*. *Dev*
605 *Neurobiol* 72:729–742. <https://doi.org/10.1002/dneu.20982>

606 Stieb SM, Muenz TS, Wehner R, Rössler W (2010) Visual experience and age affect synaptic
607 organization in the mushroom bodies of the desert ant *Cataglyphis fortis*. *Dev Neurobiol*
608 70:408–423. <https://doi.org/10.1002/dneu.20785>

609 Stöckl A, Heinze S, Charalabidis A, et al (2016) Differential investment in visual and olfactory
610 brain areas reflects behavioural choices in hawk moths. *Sci Rep* 6:1–10.
611 <https://doi.org/10.1038/srep26041>

612 Strausfeld NJ (1989) Beneath the Compound Eye: Neuroanatomical Analysis and Physiological
613 Correlates in the Study of Insect Vision. In: *Facets of Vision*. Springer, Berlin, Heidelberg,
614 pp 317–359

615 Streinzer M, Brockmann A, Nagaraja N, Spaethe J (2013) Sex and caste-specific variation in
616 compound eye morphology of five honeybee species. *PLoS One* 8:1–9.
617 <https://doi.org/10.1371/journal.pone.0057702>

618 Taylor GJ, Tichit P, Schmidt MD, et al (2019) Bumblebee visual allometry results in locally
619 improved resolution and globally improved sensitivity. *Elife* 8:1–32.
620 <https://doi.org/10.7554/eLife.40613>

621 Team RC (2016) R: A Language and Environment for Statistical Computing. R Found. Stat.
622 Comput.

623 V. R. M. Muggeo (2008) segmented: An R Package to Fit Regression Models with Broken-Line
624 Relationships. *R News* 3:343–4. <https://doi.org/10.1159/000323281>

625 van Breda JM, Stradling DJ (1994) Mechanisms affecting load size determination in *Atta*
626 *cephalotes* L. (Hymenoptera, Formicidae). *Insectes Soc* 41:423–435.

627 <https://doi.org/10.1007/BF01240645>

628 Vick K (2005) Use of multiple cues for navigation by the leaf-cutter ant *Atta cephalotes*.
629 University of Maryland, College Park, MD

630 Vilela EF, Jaffé K, Howse PE (1987) Orientation in leaf-cutting ants (Formicidae: Attini). *Anim*
631 *Behav* 35:1443–1453. [https://doi.org/10.1016/S0003-3472\(87\)80017-9](https://doi.org/10.1016/S0003-3472(87)80017-9)

632 Warrant EJ (2008) Seeing in the dark: Vision and visual behaviour in nocturnal bees and wasps.
633 *J Exp Biol* 211:1737–1746. <https://doi.org/10.1242/jeb.015396>

634 Wehner R (2003) Desert ant navigation: How miniature brains solve complex tasks. *J Comp*
635 *Physiol A Neuroethol Sensory, Neural, Behav Physiol* 189:579–588.
636 <https://doi.org/10.1007/s00359-003-0431-1>

637 Wetterer JK (1991) Allometry and the geometry of leaf-cutting in *Atta cephalotes*. *Behav Ecol*
638 *Sociobiol* 29:347–351. <https://doi.org/10.1007/BF00165959>

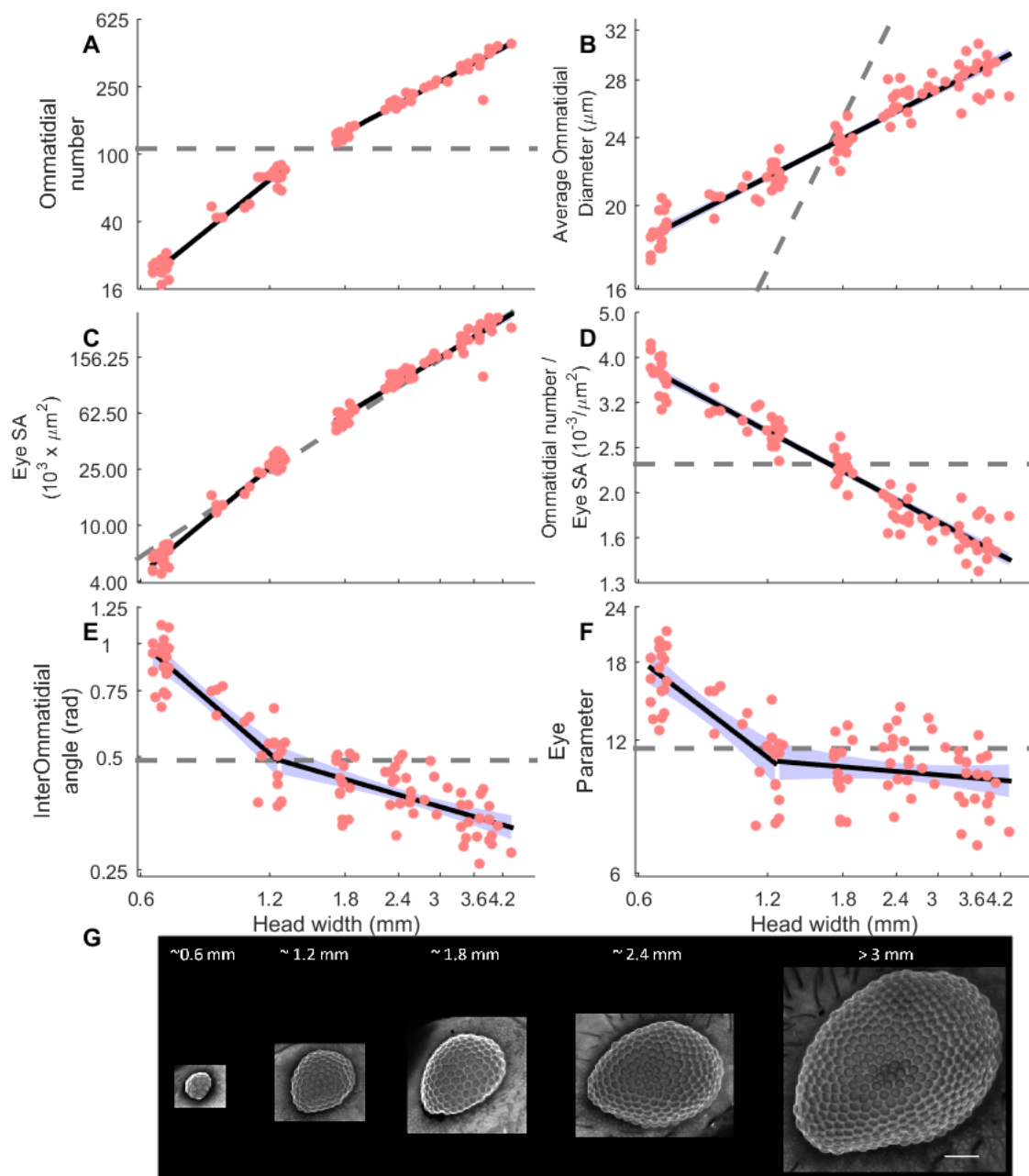
639 Wilson EO (1980) Caste and division of labor in leaf-cutter ants (Hymenoptera: Formicidae:
640 *Atta*): II. The ergonomic optimization of leaf cutting. *Behav Ecol Sociobiol* 7:57–165

641 Yilmaz A, Aksoy V, Camlitepe Y, Giurfa M (2014) Eye structure, activity rhythms, and
642 visually-driven behavior are tuned to visual niche in ants. *Front Behav Neurosci* 8:1–9.
643 <https://doi.org/10.3389/fnbeh.2014.00205>

644 Yilmaz A, Lindenberg A, Albert S, et al (2016) Age-related and light-induced plasticity in opsin
645 gene expression and in primary and secondary visual centers of the nectar-feeding ant
646 *Camponotus rufipes*. *Dev Neurobiol* 76:1041–1057. <https://doi.org/10.1002/dneu.22374>

647 Zeil J, Ribi WA, Narendra A (2014) Polarisation vision in ants, bees and wasps. In: *Polarized*
648 *Light and Polarization Vision in Animal Sciences*, Second Edition

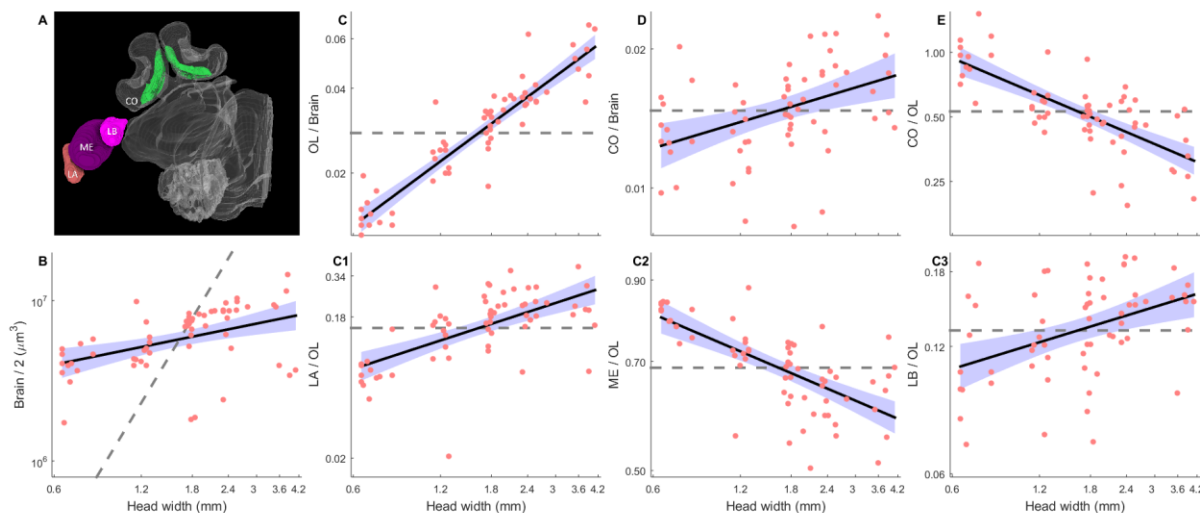
649



650
651 **Figure 1: Compound eye structure in polymorphic *A. cephalotes* workers.** **A.** Log-log plot of
652 the ommatidia number as a function of worker HW showing a significant change of slope at
653 1.38mm. **B.** Log-log plot of average ommatidial diameter as a function of worker HW. **C.** Log-
654 log plot of the eye surface area (SA) as a function of worker HW showing a significant change of
655 slope at 1.44mm. **D.** Log-log plot of ommatidia density (ommatidial number/eye SA) as a
656 function of worker HW. **E.** Log-log plot of the interommatidial angle (rad) as a function of
657 worker HW showing a significant change of slope at 1.25mm. **F** Log-log plot of the eye
658 parameter as a function of worker HW (significant change of slope at 1.26mm). **G.** Z-projections

659 of confocal images of eyes from workers with variable HW (scale bar=100 μ m). A-F: Each pink
660 point represents a single eye. Solid (significantly different from isometry) or dashed (not
661 significantly different from isometry) black lines show linear regression or piecewise linear
662 regressions as appropriate. Purple patches represent 95% confidence intervals of regression lines.
663 Dashed grey lines are the best-fitting isometric regression models.

664



665

666 **Figure 2: Volumes of polymorphic *A. cephalotes* worker brains and brain compartments.**
667 **A.** 3D reconstruction of the brain hemisphere of an *A. cephalotes* worker (HW ~4mm). **B.** Log-
668 log plot of hemisphere brain volume as a function of worker HW. **C.** Log-log plot of relative OL
669 volume as a function of worker HW. **C1.** Log-log plot of relative volume of OL lamina as a
670 function of worker HW. **C2.** Log-log plot of relative volume of OL medulla as a function of
671 worker HW. **C3.** Log-log plot of relative volume of OL lobula as a function of worker HW. **D.**
672 Log-log plot of relative MB collar volume as a function of worker HW. **E.** Log-log plot of MB
673 collar: OL volume ratio as a function of worker HW. B-E: Legend as in figure 1.
674